Simultaneous para-ferrimagnetic, metal-insulator, and orthorhombic-monoclinic transitions in $YBaCo_2O_{5.50}$

Jessica Padilla-Pantoja, Carlos Frontera, Oscar Castaño,* and José Luis García-Muñoz
Institut de Ciència de Materials de Barcelona, CSIC, Campus Universitari de Bellaterra, E-08193 Bellaterra, Spain
(Received 8 March 2010; published 28 April 2010)

Ultrahigh resolution synchrotron x-ray powder diffraction shows up two structural transitions in the layered cobaltite $YBaCo_2O_{5.50}$. The room-temperature orthorhombic structure transforms, on cooling below $T_{MI} \simeq 295$ K, to monoclinic coinciding with the apparition of a ferromagnetic moment and the occurrence of the metal to insulator transition. On further cooling, the ferromagnetic component disappears and orthorhombic symmetry is recovered.

DOI: 10.1103/PhysRevB.81.132405 PACS number(s): 71.30.+h, 75.47.Lx, 75.30.Kz, 75.25.Dk

I. INTRODUCTION

Orbital degrees of freedom play a major role in many transition-metal oxides. Cobalt oxides are very good examples of how the behavior of these degrees of freedom can influence the macroscopic properties. The fact that Co ions can easily present, in the perovskite structure, different spin states makes this interdependence even more prominent than in other transition-metal oxides such as manganites or cuprates. Layered cobaltites of the type $RBaCo_2O_{5+\delta}$ ($R \equiv$ rare earth, Y; $0 \leq \delta \leq 1$) are complex systems that present intriguing phenomena such as charge ordering, metal-insulator transitions (MITs), large thermoelectric power, transitions between complex ordered magnetic structures, spin-state transitions, fast oxygen diffusion at relatively low temperatures, mixed conductor behavior, etc.[1–17]

Intense research efforts have been made with the aim of characterizing and understanding the behavior of $RBaCo_2O_{5.50}$ ($\delta=0.50$) subfamily. These compounds present a well-known ordered structure in which pentacoordinated and hexacoordinated Co^{3+} ions form alternating planes along the y direction in a 1:1 relation. At a certain temperature, T_{MI}, they present a metal ($T > T_{MI}$) to insulator ($T < T_{MI}$) transition (MIT) accompanied by a structural transition and an anomalous cell variation. On cooling from T_{MI}, a series of complex and very intriguing magnetic transitions take place. First, a net ferromagnetic (FM) moment appears in the dc magnetization curves. This FM moment is only present for a short temperature interval and it quickly disappears on further cooling. Neutron-diffraction data evidence that the measured FM signal must come from a canted antiferromagnetic (AFM) or from a ferrimagnetic (FI) order. Furthermore, the disappearance of FM signal coincides with a change in the AFM ordered structure. A third magnetic transition has been evidenced by neutron diffraction in small rare earths such as Tb and Y.[14,18,19] This third magnetic transition is apparently absent for large rare earths (Pr, Nd).[8,18,20]

MIT is accompanied by a structural phase transition characterized by a strongly anisotropic evolution of cell parameters and a discontinuity of the unit-cell volume. In most of the cases, cell volume is larger in the conducting phase ($T > T_{MI}$) due to the expansion of CoO_6 octahedra (while the volume of CoO_5 pyramids shrinks).[5,7,20] This asymmetric behavior of the average Co-O bond distances was initially interpreted as a change in the spin state of Co in octahedral sites.[7] However, cell volume of $HoBaCo_2O_{5.50}$ behaves in the opposite way across MIT.[21,22] It must be mentioned that for Ho MIT coincides with the onset of the FM moment while for larger rare earths, these two transition are clearly separated.

The origin of the FM moment appearing only within a very short temperature interval has been the subject of a vivid interest during last years. Symmetry analysis[14–16] predicts that FM must come from a FI structure likely related with a doubling of the cell along x direction with respect to the cell above the MIT. Different diffraction measurements made on single-crystal samples have confirmed the doubling of a-lattice parameter below T_{MI}.[23,24] In contrast, this doubling has been not clearly seen in powder samples.[16]

In this work, we present the results of a detailed structural study on $YBaCo_2O_{5.50}$ showing great coincidences with the behavior of $HoBaCo_2O_{5.50}$. These are the unique two known cases in which the MIT coincides with the onset of the FM phase. We have found that the evolution of the unit-cell volume is the opposite to the larger rare-earths case (Tb, Gd, Nd, Pr, …) as it expands when cooling across the transition, in accordance with Ho case.[21,25] We also find that coinciding with the MIT and the onset of the FM phase, the crystal system changes from orthorhombic ($T > T_{MI}$) to monoclinic ($T < T_{MI}$). On further cooling, and below the disappearance of the FM phase, the orthorhombic cell is apparently recovered.

II. EXPERIMENTAL

Initial $YBaCo_2O_{5+\delta}$ sample was prepared by sol-gel method as reported elsewhere.[18] To correct oxygen stoichiometry of the as-sintered specimen, we annealed it, mostly in powder form, under oxygen atmosphere at 290 °C during 40 h and slowly cooled it to RT at 5 °C/h. X-ray diffraction showed a single-phased material (homogeneous oxygen content/ordering). Cell parameters obtained fairly coincide with those previously reported for $YBaCo_2O_{5.50}$.[26]

dc magnetization has been measured using a superconducting quantum interferometer device (SQUID, Quantum Design) with an applied field of 0.5 T after cooling under the applied field. dc resistance has been measured by the four-

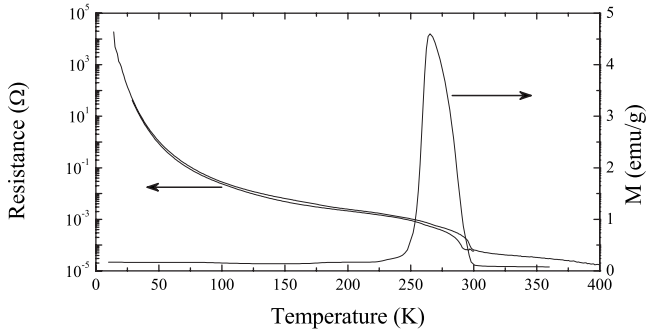

FIG. 1. dc resistivity (left axis) and dc magnetization measured under an applied field of 5000 Oe (right axis) of the prepared $YBaCo_2O_{5.50}$ sample.

probe method using a physical properties measurement system (PPMS, Quantum Design).

The structural study has been carried out using synchrotron x-ray powder diffraction (SXRPD) at ID31 beamline of ESRF (Grenoble, France). A short wavelength $\lambda=0.39978(25)$ Å, to reduce the absorption, was selected with a double-crystal Ge (111) monochromator and calibrated with Si NIST ($a=5.43094$ Å). Optimum transmission was achieved by enclosing the finely grounded sample in a 0.5-mm-diameter borosilicate glass capillary, and appropriate spinning of the capillary in the beam ensured for a good powder averaging. Diffraction data has been analyzed with the Rietveld method using FULLPROF suite of programs.[27] Low-temperature patterns down to 5 K were recorded placing the capillary in a continuous liquid-helium-flow cryostat with rotating sample rod. Measurements above RT (up to 350 K) have been done by using a hot air blower.

III. RESULTS AND DISCUSSION

dc resistance and magnetization (plotted in Fig. 1) show the expected behavior for this compound. On cooling, the upturn of the resistivity (MIT) and the magnetization coincide at $T_{MI}\simeq 295$ K. The magnetic moment reaches its maximum value at $T_2\simeq 265$ K and vanishes quickly on cooling below this temperature. This second transition is rounded in samples with oxygen content slightly above the optimal one ($\delta=0.52$),[26] thus, the sharpness of the transitions in Fig. 1 indicates that our sample is well crystallized, with the correct oxygen stoichiometry and an optimal vacancy ordering.[28,29]

SXRPD patterns collected above RT can be refined using *Pmmm* (no. 47) space group (SG) with the standard $a_p\times 2a_p\times 2a_p$ cell. In contrast, pattern collected at 290 K reveals a subtle but well-resolved splitting of (h k l) peaks with $h\neq 0$ and $k\neq 0$. This splitting is also present in patterns collected at $T=270$ and 245 K but it disappears at 210 and 5 K. This is illustrated in Fig. 2, showing the splitting of (1 2 0) reflection into ($\bar{1}$ 2 0)-(1 2 0).

On another hand, diffraction on single crystals reported the apparition, coinciding with the MIT, of a superstructure doubling a-lattice parameter and described the structure using *Pmma* (no. 51) SG.[23,24] In the view of the monoclinic

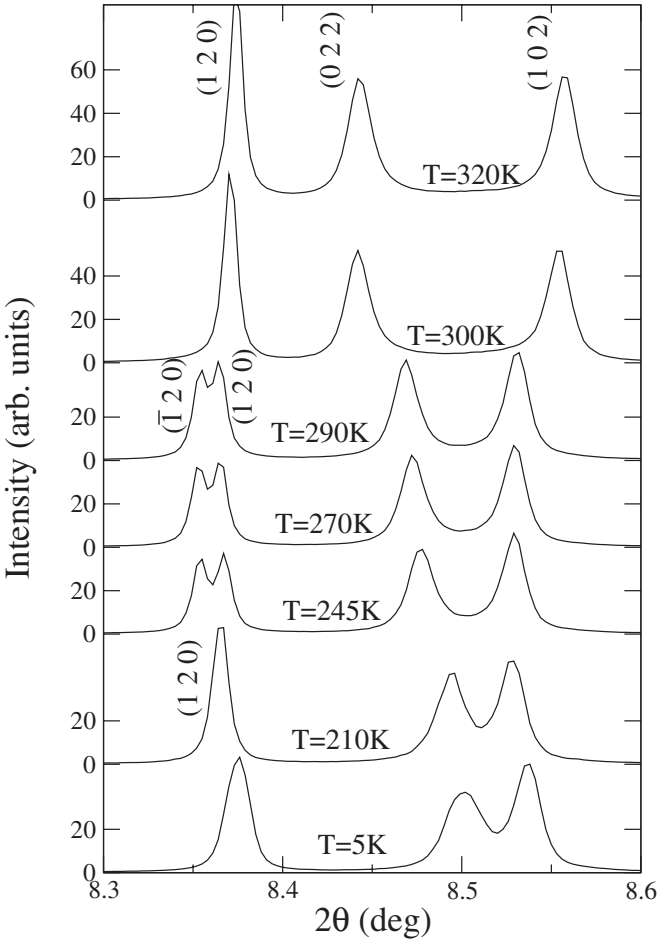

FIG. 2. Selected portion of the SXRPD measured at indicated temperatures. Reflections are indexed on the basis of $a_p\times 2a_p\times 2a_p$ lattice. Diffraction patterns have been shifted up for clarity. The splitting of (1 2 0) reflection into ($\bar{1}$ 2 0)-(1 2 0) can be clearly appreciated for patterns collected at $T=290$, 270, and 245 K. This splitting is absent at $T=210$ and 5 K.

cell, this space group must be ruled out for $YBaCo_2O_{5.50}$. In order to refine the structure, we first attempted to use the $P112/m$ (no. 10) SG (and $a_p\times 2a_p\times 2a_p$ cell), reported in Ref. 25, with very good results ($\chi^2=4.0$; $R_B=3.4\%$). In a second attempt, we tested $P112/a$ (no. 13) and $a\sim 2a_p$. The obtained agreement parameters are almost identical ($\chi^2=3.9$; $R_B=3.4\%$). In order to discriminate which description must be taken, we carefully examined the diffraction patterns collected below T_{MI} to find a further confirmation of $2a_p\times 2a_p\times 2a_p$ lattice. SXRPD patterns display few tiny peaks that confirm this lattice as illustrated in Fig. 3. Thus, we must conclude that the structure of $YBaCo_2O_{5.50}$, in this temperature region, must be described using $P112/a$ SG and $2a_p\times 2a_p\times 2a_p$ cell. Table I lists the structural details obtained using this description at $T=270$ K.

Neutron powder diffraction has evidenced that the second (on cooling) magnetic transition at $T_2\simeq 265$ K is due to the formation of a purely AFM structure that doubles c-lattice parameter (magnetic lattice).[14,16,20,30] Across this transition, we cannot appreciate any structural change. In contrast, we observe a second structural transition between 210 and

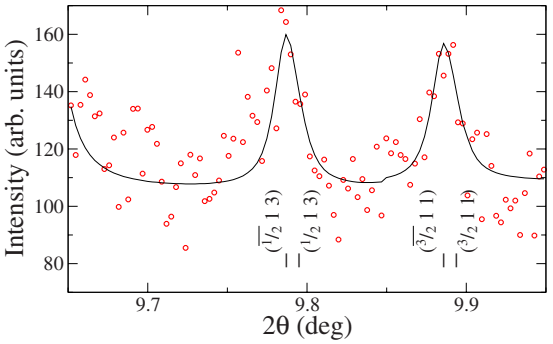

FIG. 3. (Color online) Selected portion of the Rietveld refinement of SXRPD pattern measured at 270 K and indexed according to $a_p \times 2a_p \times 2a_p$ cell.

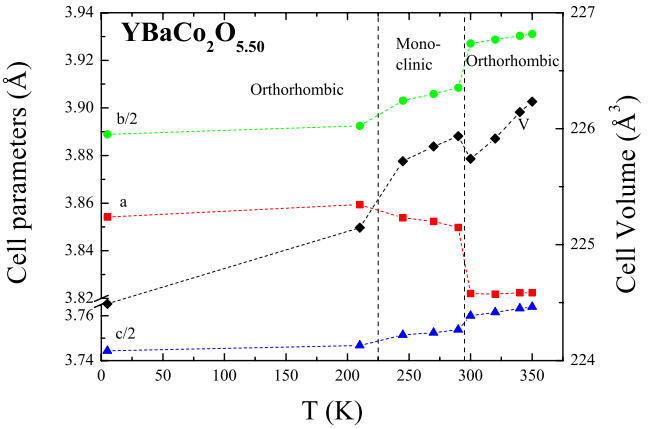

FIG. 4. (Color online) Evolution with temperature of a, b, and c cell parameters (left axis) and unit-cell volume (right axis) obtained by Rietveld refinement of SXRPD patterns. Cell parameters are referred to $a_p \times 2a_p \times 2a_p$ setting. The values of the monoclinic angle obtained are γ=90.074(2)°, 90.085(2)°, and 90.093(2)° for T=290 K, 270 K, and 245 K, respectively.

245 K. In this temperature region, $YBaCo_2O_{5.50}$ presents the third magnetic transition ($T_3 \simeq 230$ K).[18] Below this transition, the cell becomes orthorhombic (up to the resolution we have), there is an anisotropic variation in cell parameters and an anomalous contraction of the cell volume. These effects are shown in Fig. 4 that plots the evolution of cell parameters and cell volume (referred to $a_p \times 2a_p \times 2a_p$ setting). It is worth to recall that cell volume enlarges when entering the insulating phase (cooling across T_{MI}). This behavior coincides with that reported for $HoBaCo_2O_{5.50}$ but is opposite to that found for larger rare earths (Tb, Gd, Nd, Pr, …). Therefore, to be highlighted is that the unit-cell volume contracts at T_3 instead of at T_{MI}.

From symmetry considerations, Plakhty *et al.*[14] proposed that, below T_3, the crystal structure must change to *Pcca* (no. 54) and c-lattice parameter must be $c \sim 4a_p$. Thus, our results indicate that (in $YBaCo_2O_{5.50}$) the third magnetic transition is concomitant with an structural transition characterized by a change from a monoclinic ($T > T_3$) to a orthorhombic ($T < T_3$) crystal system. The doubling of c-lattice parameter would help to understand this symmetry change.

IV. CONCLUSIONS AND SUMMARY

Variations in the physical properties of $RBaCo_2O_{5.50}$ layered cobaltites by introducing A-site cations of progressively smaller sizes were previously signaled by several groups (e.g., in Refs. 18, 20, and 21). Interestingly, the MIT is present for all the lanthanides investigated, as well as successive magnetic transitions of the type PM→FM→AFM upon cooling. However, the number of structural transitions and magnetic orderings depends on the rare-earth size. A precise description of the structural changes is key to shed light on the physical origin(s) of the MIT detected with different rare earths and must help to discern between the different mechanisms proposed (spin-state change, orbital order, and charge transfer). For that an accurate location of oxygen atoms is required.

TABLE I. Structure at 270 K refined using SG $P112/a$ (no. 13). Lattice parameters are a=7.7046(1), b=7.8120(1), c=7.5052(1), and γ=90.082(2)°. Agreement parameters are χ^2=3.9 and R_B=3.4%.

Atom	W.P.	x/a	y/b	z/c	β_{iso}
Ba	4*g*	−0.0003(2)	0.2492(1)	−0.0010(5)	0.59(1)
Y	4*g*	0.0010(3)	0.2714(1)	0.4982(8)	0.73(2)
Co_{P_1}	2*e*	1/4	0	0.258(3)	0.58(3)
Co_{P_2}	2*e*	1/4	0	0.743(3)	0.58(3)
Co_{O_1}	2*f*	1/4	1/2	0.249(3)	0.37(4)
Co_{O_2}	2*f*	1/4	1/2	0.743(3)	0.37(4)
O1	2*e*	1/4	0	0.000(9)	1.3(2)
O2	2*f*	1/4	1/2	0.000(9)	1.3(2)
O3	2*f*	1/4	1/2	0.500(9)	1.3(2)
O4	4*g*	−0.009(5)	0.014(5)	0.318(4)	0.8(2)
O5	4*g*	0.002(7)	0.488(5)	0.278(4)	0.8(2)
O6	4*g*	0.264(4)	0.235(5)	0.290(5)	0.8(2)
O7	4*g*	0.741(4)	0.244(5)	0.305(5)	0.8(2)

Making R=Y or Ho in $RBaCo_2O_{5.5}$, the MIT coincides with the Curie temperature and the PM to FI transition (PM→FM). We have confirmed for R=Y that, in contrast with the case of lanthanides of bigger size (such as Gd, Pr, or La),[7,20,31] the cell volume enlarges in the insulating phase across MIT. In agreement with the behavior reported for Ho (with very similar cation size),[25] we have detected a crystal system change from orthorhombic to monoclinic on cooling across T_{MI} and its coincidence with the onset of FM moment. In $YBaCo_2O_{5.50}$, electron localization is accompanied by a structural transformation toward a $P112/a$ ($2a_p \times 2a_p \times 2a_p$) cell in the ferrimagnetic-insulating phase. Other SG and symmetries previously proposed ($Pmma$ and $P112/m$) have been ruled out. The monoclinic angle found, that is very close to 90° ($\gamma \simeq 90.09°$), signals the electronic perhaps also magnetic origin of the symmetry and cell dimension changes. Therefore, a main conclusion from present work is that in the case of $YBaCo_2O_{5.50}$, the ferrimagnetic order (only present in a narrow temperature interval near room temperature) appears in a monoclinic $P112/a$ structure (described in Table I) that also doubles the a axis. Furthermore, we have observed that the new monoclinic phase is not stable at low temperatures and $YBaCo_2O_{5.50}$ undergoes a second structural transformation below 245 K. Further studies are in progress to provide a more accurate description of the successive structures detected in $YBaCo_2O_{5.50}$ and to clarify the relationship between the electronic and successive structural and magnetic transitions in this appealing cobalt oxide.

ACKNOWLEDGMENTS

Financial support was received from MICINN (Spanish government) under Projects No. MAT2006-11080-C02-02, No. MAT2009-09308, and NANOSELECT No. CSD2007-00041. We thank European Synchrotron Radiation Facility for the provision of beam time, and M. Brunelli for her assistance during data collection.

*Present address: Institut de Bioenginyeria de Catalunya, c/Baldiri Reixac 13, 08028 Barcelona, Spain.

[1] I. O. Troyanchuk, N. V. Kasper, D. D. Khalyavin, H. Szymczak, R. Szymczak, and M. Baran, Phys. Rev. Lett. **80**, 3380 (1998).
[2] A. Maignan, C. Martin, D. Pelloquin, N. Nguyen, and B. Raveau, J. Solid State Chem. **142**, 247 (1999).
[3] T. Vogt, P. M. Woodward, P. Karen, B. A. Hunter, P. Henning, and A. R. Moodenbaugh, Phys. Rev. Lett. **84**, 2969 (2000).
[4] E. Suard, F. Fauth, V. Caignaert, I. Mirebeau, and G. Baldinozzi, Phys. Rev. B **61**, R11871 (2000).
[5] H. Kusuya, A. Machida, Y. Moritomo, K. Kato, E. Nishibori, M. Takata, M. Sakata, and A. Nakamura, J. Phys. Soc. Jpn. **70**, 3577 (2001).
[6] M. Respaud, C. Frontera, J. L. García-Muñoz, Miguel Ángel G. Aranda, B. Raquet, J. M. Broto, H. Rakoto, M. Goiran, A. Llobet, and J. Rodríguez-Carvajal, Phys. Rev. B **64**, 214401 (2001).
[7] C. Frontera, J. L. García-Muñoz, A. Llobet, and M. A. G. Aranda, Phys. Rev. B **65**, 180405(R) (2002).
[8] F. Fauth, E. Suard, V. Caignaert, and I. Mirebeau, Phys. Rev. B **66**, 184421 (2002).
[9] J. C. Burley, J. F. Mitchell, S. Short, D. Miller, and Y. Tang, J. Solid State Chem. **170**, 339 (2003).
[10] A. A. Taskin, A. N. Lavrov, and Y. Ando, Proceedings of the 22nd International Conference on Thermoelectrics, 2003 (IEEE, New York, 2003), p. 196.
[11] A. A. Taskin, A. N. Lavrov, and Y. Ando, Phys. Rev. Lett. **90**, 227201 (2003).
[12] D. D. Khalyavin, S. N. Barilo, S. V. Shiryaev, G. L. Bychkov, I. O. Troyanchuk, A. Furrer, P. Allenspach, H. Szymczak, and R. Szymczak, Phys. Rev. B **67**, 214421 (2003).
[13] A. A. Taskin, A. N. Lavrov, and Y. Ando, Phys. Rev. B **71**, 134414 (2005).
[14] V. P. Plakhty, Y. P. Chernenkov, S. N. Barilo, A. Podlesnyak, E. Pomjakushina, E. V. Moskvin, and S. V. Gavrilov, Phys. Rev. B **71**, 214407 (2005).
[15] D. D. Khalyavin, Phys. Rev. B **72**, 134408 (2005).
[16] D. D. Khalyavin, D. N. Argyriou, U. Amann, A. A. Yaremchenko, and V. V. Kharton, Phys. Rev. B **75**, 134407 (2007).
[17] C. Frontera, A. Caneiro, A. E. Carrillo, J. Oró-Solé, and J. L. García-Muñoz, Chem. Mater. **17**, 5439 (2005).
[18] C. Frontera, J. L. García-Muñoz, and O. Castaño, J. Appl. Phys. **103**, 07F713 (2008).
[19] D. D. Khalyavin, D. N. Argyriou, U. Amann, A. A. Yaremchenko, and V. V. Kharton, Phys. Rev. B **77**, 064419 (2008).
[20] C. Frontera, J. L. García-Muñoz, A. E. Carrillo, M. A. G. Aranda, I. Margiolaki, and A. Caneiro, Phys. Rev. B **74**, 054406 (2006).
[21] E. Pomjakushina, K. Conder, and V. Pomjakushin, Phys. Rev. B **73**, 113105 (2006).
[22] J.-E. Jørgensen and L. Keller, Phys. Rev. B **77**, 024427 (2008).
[23] D. Chernyshov, V. Dmitriev, E. Pomjakushina, K. Conder, M. Stingaciu, V. Pomjakushin, A. Podlesnyak, A. A. Taskin, and Y. Ando, Phys. Rev. B **78**, 024105 (2008).
[24] Yu. P. Chernenkov, V. P. Plakhty, V. I. Fedorov, S. N. Barilo, S. V. Shiryaev, and G. L. Bychkov, Phys. Rev. B **71**, 184105 (2005).
[25] L. Malavasi, M. Brunelli, Y. Diaz-Fernandez, B. Pahari, and P. Mustarelli, Phys. Rev. B **80**, 153102 (2009).
[26] D. Akahoshi and Y. Ueda, J. Solid State Chem. **156**, 355 (2001).
[27] J. Rodríguez-Carvajal, Physica B **192**, 55 (1993).
[28] C. Frontera, J. L. García-Muñoz, O. Castaño, C. Ritter, and A. Caneiro, J. Phys.: Condens. Matter **20**, 104228 (2008).
[29] D. Akahoshi and Y. Ueda, J. Phys. Soc. Jpn. **68**, 736 (1999).
[30] D. P. Kozlenko, Z. Jirák, N. O. Golosova, and B. N. Savenko, Eur. Phys. J. B **70**, 327 (2009).
[31] E.-L. Rautama, V. Caignaert, P. Boullay, A. K. Kundu, V. Pralong, M. Karppinen, C. Ritter, and B. Raveau, Chem. Mater. **21**, 102 (2009).